Molecular Dynamics Simulation of the Consequences of a *PYCR1* Mutation (p.Ala189Val) in Patients with Complex Connective Tissue Disorder and Severe Intellectual Disability

Journal of Investigative Dermatology (2017) **137,** 525–528; doi:10.1016/j.jid.2016.10.007

TO THE EDITOR

Heritable connective tissue disorders are a phenotypically highly heterogeneous group of conditions with a spectrum of manifestations affecting different organs and tissues. The heterogeneity is explained primarily by the repertoire of individual genes harboring mutations in these conditions (Uitto, 2014). As examples of the clinical heterogeneity with tissue specific connective tissue manifestations are as follows: (i) Cutis laxa (CL), characterized by redundant, loose, and sagging skin with loss of recoil. Extracutaneous manifestations include cardiac, arterial, pulmonary, and gastrointestinal abnormalities, and the clinical findings are due to mutations in the genes required for synthesis and assembly of the elastic fiber network (Uitto et al., 2013); (ii) Ehlers-Danlos syndrome (EDS), demonstrating hyperextensible skin with recoil and loose jointedness, sometimes associated with cardiovascular manifestations. EDS is classified into six subcategories, associated with distinct mutations primarily in the genes encoding various collagens or enzymes critical for collagen biosynthesis and assembly (Byers and Murray, 2014); (iii) Osteogenesis imperfecta (OI), manifesting with fragile bones with varying degree of tendency for fractures. OI is primarily caused by mutations in the genes, proα1(I) and proα2(I), encoding type I collagen, the major matrix component in cortical bone (Forlino and Marini, 2016).

In this study, we have examined the molecular basis of connective tissue manifestations, including features of CL, EDS, and OI, associated with severe intellectual disability, in a consanguineous family from Iran with Persian ethnicity with five affected individuals (Figure 1a and Case Reports in Supplementary Materials online). The clinical findings included intellectual disability, triangular facies, and intrauterine growth retardation as well as wrinkled/inelastic skin and joint hypermobility, characteristic features of autosomal recessive CL due to proline synthesis defect (ARCL type 2B) (Dimopoulou et al., 2013). Histopathology of skin biopsies revealed a marked reduction in elastic fibers and marked thinning and fragmentation of few visualized elastic fibers when examined by Verhoeff-von Gieson stain (Figure 1b). A mild inflammatory cell infiltration around the papillary vessels was noted. These clinical findings, with the pedigree analysis, and lack of elastin suggested the diagnosis of autosomal recessive CL (ARCL), possibly related to *ALDH18A1* or *PYCR1* mutations in patients with ARCL type 3A and 2B (OMIM# 219150 and 612940, respectively). Different types of CL can be caused by mutations in at least nine distinct genes (Urban and Davis, 2014). This study was approved by the Institutional Review Board of Pasteur Institute of Iran, and the patients, their parents or guardians gave their informed written consent to participate in this study and gave permission to use their photos/case history to be published.

The initial approach to identify candidate genes in this family was to perform whole genome-wide single-nucleotide polymorphism-based homozygosity mapping using Illumina Infinum Exome-24 Bead Chip (240,000 single-nucleotide polymorphism markers) (Illumina, San Diego, CA), which revealed conserved homozygosity blocks along the entire autosome (Figure 1c). After elimination of potentially incidental runs of homozygosity (less than 2 Mb), the nine candidate genes related to ARCL were superimposed with homozygosity blocks that identified three potential candidate genes: *GORAB*, *FBLN4*, and *PYCR1*. *GORAB* is associated with gerodermia osteodysplastica characterized by wrinkly skin and osteoporosis, features shown by our patients (Yildirim et al., 2011). However, sequencing of *GORAB* and *FBLN4* did not reveal any pathogenic sequence variants.

Mutation analysis of *PYCR1* was performed by PCR amplification followed by bidirectional Sanger sequencing. Sequencing identified a homozygous c.566C>T, p.Ala189Val (accession no. NM_006907) mutation in *PYCR1* segregating in the family with the affected individuals (Figure 1b). In 2009, two independent groups showed pathogenic mutations in *PYCR1* in ARCL type 2B, including p.Ala189Val in a patient from Oman initially diagnosed as gerodermia osteodysplastica (Guernsey et al., 2009; Reversade et al., 2009). This finding highlights the clinical overlap between gerodermia osteodysplastica and ARCL type 2B (Yildirim et al., 2011). Up to now, 34 pathogenic mutations have been reported in this gene, about half of them being missense.

Abbreviations: ARCL, autosomal recessive CL; CL, cutis laxa; EDS, Ehlers-Danlos syndrome; MD, molecular dynamics; OI, osteogenesis imperfecta

Accepted manuscript published online 15 October 2016; corrected proof published online 5 December 2016

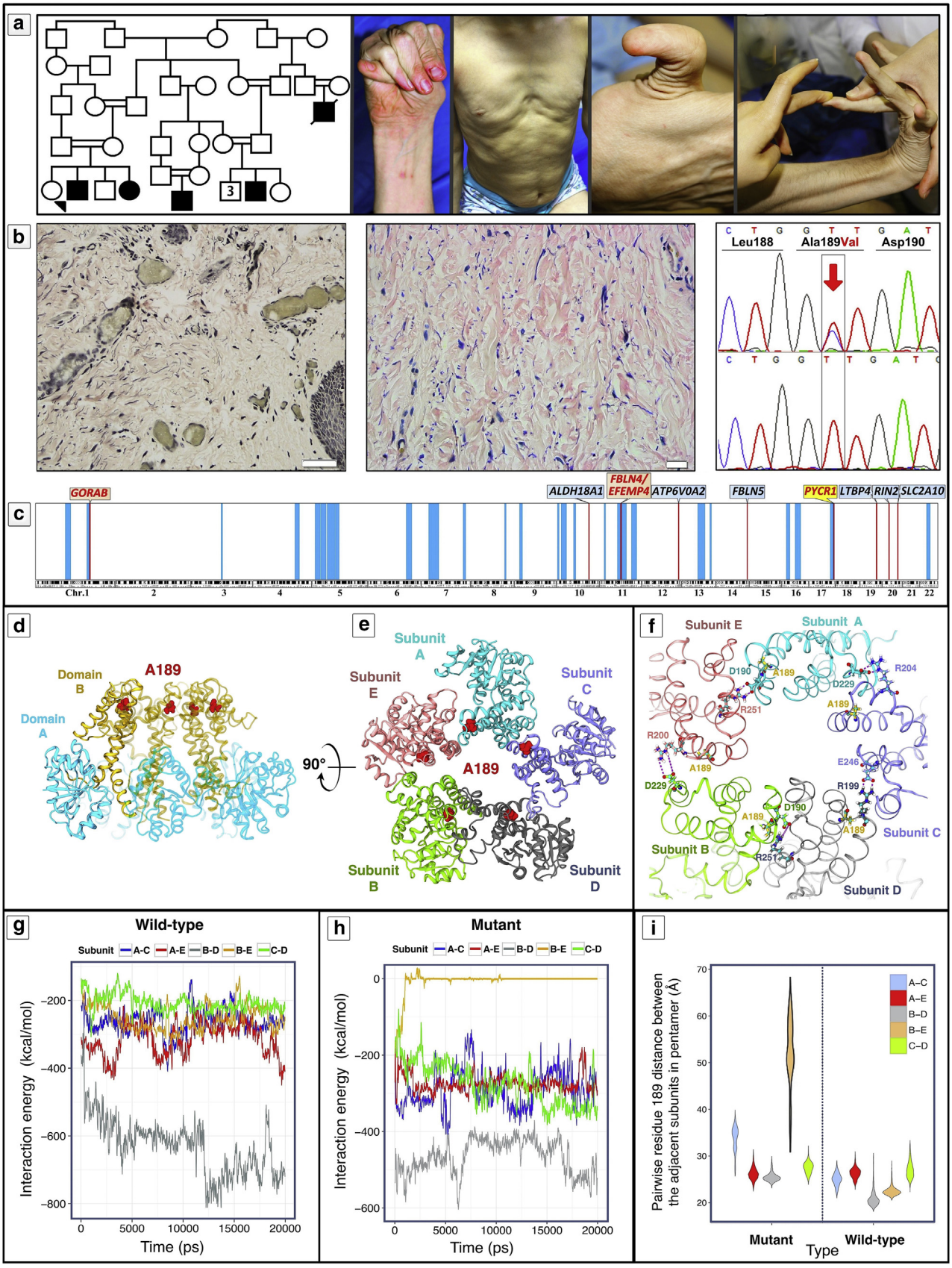

Figure 1. Clinical features, homozygosity mapping, and *in silico* analysis of the consequences of the p.Ala189Val mutation in *PYCR1*. (**a**) Family pedigree and clinical characteristics; (**b**) histopathology, and mutation analysis of *PYCR1* in the proband (lower panel) and in a heterozygous parent (upper panel) in consanguineous extended family (scale bars = 50 μm and 20 μm for the left and right histopathology slides, respectively); (**c**) genome-wide SNP-based homozygosity mapping identified candidate genes for mutation analysis; (**d**) front and (**e**) top view of the pentameric assembly of the PYCR1 complex; (**f**) a

The *PYCR1* gene encodes pyrroline-5-carboxylate reductase, a mitochondrial enzyme that catalyzes the final step of proline biosynthesis and reduces pyrroline-5-carboxylate to L-proline. Full-length PYCR1 polypeptide folds into two separate domains forming a monomeric complex structure (Figure 1d). The N-terminal domain (N) contains the catalytic site, whereas the C-terminal domain (C) is mainly involved in multimerization. The complex of *PYCR1* is a pentamer, comprising five polypeptide subunits (A–E) (Figure 1e), two of which together form decameric "yo-yo-like" architecture. Each decameric complex is built from two identical interacting pentamers through their C domains (Supplementary Figure S1a online).

To examine the consequences of the p.Ala189Val mutation at the molecular level, we utilized the time-course computational method, the molecular dynamics (MD) simulation, to investigate the structural impact of this mutation and its dynamic influence on multimeric stability and subunit motions of the PYCR1 complex. MD simulation provides a detailed description of atomic motions of protein as a function of time by solving Newton's equation of motions of classical physics (Karplus and McCammon, 1986). Crystal structures of PYCR1 complexes (Protein Data Bank entries: 2GRA and 2IZZ) were used as the initial conformations for all analyses (Meng et al., 2006). After preparation of wild-type (Ala189) and mutant (Val189) structures, MD simulations were performed by the generalized born implicit solvent method of the NAMD 2.10 package (Phillips et al., 2005) for the total production run of 20 ns, and the data were analyzed in R statistical language (for detailed information about the MD protocol, see Supplementary Materials). All computational analyses were also accomplished for one of the dimers in decameric conformation to confirm the structural impact of mutation in different multimeric states of PYCR1 (see Supplementary Materials for more information about related results).

Initial structural analysis showed that p.Ala189Val mutation is located at the end of Helix-9 within the C-terminal domain of each PYCR1 subunit, which suggested the possible interference of multimeric assembly by this mutation. To verify this assumption, MD simulations in the wild-type and mutant structures in pentameric conformations were performed (thermodynamic parameters during the MD simulation were monitored and reported in Supplementary Table S1 online). During the monitoring of the 20-ns MD simulations, we observed that the B and E subunits were separated from each other in mutant conformation, which resulted in disassembly of the complex within less than 1 ns. In contrast, in this time period, the wild-type structure stayed assembled (Movie S1). For further analysis, some key structural parameters, including the average distance between the backbone atoms (root mean square deviations) of each subunit, pairwise-distance distribution of Ala189 (in wild-type) and Val189 (mutant), and the interaction energy between the adjacent subunits in wild-type and mutant PYCR1 complexes, were measured for all 4,000 structural snapshots (Figure 1g and h). Initial structural analysis including the root mean square deviation fluctuation between wild-type and mutant conformations during the MD simulation indicated that p.Ala189Val mutation affects the C-terminal rather than the N-terminal region of each monomer, thus confirming the effect of mutation on the dynamic behavior of C-terminus (Supplementary Figure S1c and d; see Supplementary Materials for full description). The pairwise-distance distribution of Ala189 and Val189 between the adjacent subunits of mutant and wild-type conformations indicated that the Val189 distance distribution between the B and E subunits was increased in comparison with the wild-type, which confirmed that the B and E subunits gradually drifted away (Figure 1i). Moreover, the interaction energy between the B and E subunits progressively diminished within the first 1,000 ps of simulation in the mutant pentameric structure, whereas it remained steady in the wild-type structure (Figure 1g and h). This was also detectable between the B and D subunits in which interaction energy between subunits decreased followed by the increasing distance of mutated residues along the trajectories in the pentameric form.

To address the question of which molecular interactions are involved in disassembly of the B–E subunits, we measured the inter- and intrasubunit salt-bridge interactions and hydrogen bonds between the wild-type and mutant conformations of all snapshots. Figure 1f depicts the exclusive intersubunit salt-bridge interactions in all 2,000 sampled wild-type structures that were absent in the mutant form during the simulation. Supplementary Tables S2 and S3 online list the overall intersubunit salt-bridge and hydrogen bonds that are eliminated in p.Ala189Val mutant pentameric and decameric structures, respectively. Most of these interactions are located at the C domain responsible in the multimeric assembly of the PYCR1 complex. Moreover, this mutation affects all adjacent intersubunit interactions to weaken the multimeric assembly.

In addition to the assembly of PYCR1 to pentameric and decameric complexes, it has been recently demonstrated that PYCR1, together with PYCR2, is a component of the ribonucleotide reductase small subunit B complex, and their interactions have been suggested to protect fibroblasts from oxidative stress (Kuo et al., 2016). These mechanisms may be operative in connective tissues, and inactivation of this complex may explain the widespread deficiency manifesting as a complex disorder with features of CL, EDS, and OI, as encountered in our patients.

In summary, in this study we report a missense mutation, p.Ala189Val, in the *PYCR1* gene in a family with ARCL type 2B. In addition to CL, these patients have clinical findings consistent with EDS and OI, signifying the presence of

subset of wild-type intersubunit salt-bridge interactions (magenta dashed line) of pentameric protein that are specifically diminished in mutant form throughout the MD simulation; (**g**) wild-type and (**h**) mutant interaction energies between adjacent subunits of pentameric PYCR1; (**i**) pairwise distance distribution of residue 189 of adjacent subunits in mutant and wild-type pentameric form during the MD trajectories. MD, molecular dynamics; PYCR1, pyrroline-5-carboxylate reductase; SNP, single-nucleotide polymorphism.

a complex connective tissue disorder. In addition, the patients had severe intellectual disability that cosegregated with the connective tissue phenotype. A combination of computational methods demonstrated the impact of the missense mutation on structural stability, multimeric assembly, and dynamic behavior of the PYCR1 complex. We showed that Ala189 plays a pivotal role in maintaining the pentameric and decameric assembly of PYCR1, and that the p.Ala189Val mutation also leads to elimination of the critical inter- and intrasubunit interactions by affecting adjacent charged residues within the region in both pentameric and decameric conformations. These findings are predicted to result in loss of PYCR1 activity with severe phenotypic consequences.

CONFLICT OF INTEREST

The authors state no conflicts of interest.

ACKNOWLEDGMENT

Molecular dynamics simulation was performed using the Computing Cluster Facility of the University of Tehran, Iran. Carol Kelly assisted in manuscript preparation.

***Hassan Vahidnezhad*[1,2,10], *Razieh Karamzadeh*[3,4,10], *Amir Hossein Saeidian*[1,10], *Leila Youssefian*[1,9,10], *Soheila Sotoudeh*[5], *Sirous Zeinali*[2,6], *Mohammad Vasei*[7], *Fatemeh Golnabi*[6], *Taghi Baghdadi*[8] *and Jouni Uitto*[1,*]**

[1]*Department of Dermatology and Cutaneous Biology, Sidney Kimmel Medical College at Thomas Jefferson University, Philadelphia, USA;* [2]*Department of Molecular Medicine, Biotechnology Research Center, Pasteur Institute of Iran, Tehran, Iran;* [3]*Department of Biophysics, Institute of Biochemistry and Biophysics, University of Tehran, Tehran, Iran;* [4]*Department of Molecular Systems Biology, Cell Science Research Center, Royan Institute for Stem Cell Biology and Technology, ACECR, Tehran, Iran;* [5]*Department of Dermatology, Children's Hospital Medical Center, Pediatric Center of Excellence, Tehran University of Medical Sciences, Tehran, Iran;* [6]*Kawsar Human Genetics Research Center, Tehran, Iran;* [7]*Department of Pathology and Digestive Disease Research Institute, Shariati Hospital, Tehran University Medical Sciences, Tehran, Iran;* [8]*Department of Orthopedic Surgery, Imam Khomeini Hospital, Tehran University of Medical Sciences, Tehran, Iran; and* [9]*Department of Medical Genetics, Tehran University of Medical Sciences, Tehran, Iran*
[10]*These authors contributed equally to this work.*
[*]*Corresponding author e-mail: Jouni.Uitto@Jefferson.edu*

SUPPLEMENTARY MATERIAL

Supplementary material is linked to the online version of the paper at www.jidonline.org, and at http://dx.doi.org/10.1016/j.jid.2016.10.007.

REFERENCES

Byers PH, Murray ML. Ehlers-Danlos syndrome: a showcase of conditions that lead to understanding matrix biology. Matrix Biol 2014;33:10–5.

Dimopoulou A, Fischer B, Gardeitchik T, Schroter P, Kayserili H, Schlack C, et al. Genotype-phenotype spectrum of PYCR1-related autosomal recessive cutis laxa. Mol Genet Metab 2013;110:352–61.

Forlino A, Marini JC. Osteogenesis imperfecta. Lancet 2016;387:1657–71.

Guernsey DL, Jiang H, Evans SC, Ferguson M, Matsuoka M, Nightingale M, et al. Mutation in pyrroline-5-carboxylate reductase 1 gene in families with cutis laxa type 2. Am J Hum Genet 2009;85:120–9.

Karplus M, McCammon JA. The dynamics of proteins. Sci Am 1986;254:42–51.

Kuo ML, Lee MB, Tang M, den Besten W, Hu S, Sweredoski MJ, et al. PYCR1 and PYCR2 interact and collaborate with RRM2B to protect cells from overt oxidative stress. Sci Rep 2016;6:18846.

Meng Z, Lou Z, Liu Z, Li M, Zhao X, Bartlam M, et al. Crystal structure of human pyrroline-5-carboxylate reductase. J Mol Biol 2006;359:1364–77.

Phillips JC, Braun R, Wang W, Gumbart J, Tajkhorshid E, Villa E, et al. Scalable molecular dynamics with NAMD. J Comput Chem 2005;26:1781–802.

Reversade B, Escande-Beillard N, Dimopoulou A, Fischer B, Chng SC, Li Y, et al. Mutations in PYCR1 cause cutis laxa with progeroid features. Nat Genet 2009;41:1016–21.

Uitto J. Heritable disorders of connective tissue: introduction to mini-review cluster. Matrix Biol 2014;33:8–9.

Uitto J, Li Q, Urban Z. The complexity of elastic fibre biogenesis in the skin—a perspective to the clinical heterogeneity of cutis laxa. Exp Dermatol 2013;22:88–92.

Urban Z, Davis EC. Cutis laxa: intersection of elastic fiber biogenesis, TGFbeta signaling, the secretory pathway and metabolism. Matrix Biol 2014;33:16–22.

Yildirim Y, Tolun A, Tuysuz B. The phenotype caused by PYCR1 mutations corresponds to geroderma osteodysplasticum rather than autosomal recessive cutis laxa type 2. Am J Med Genet A 2011;155A:134–40.

Effects of Depilation Methods on Imiquimod-Induced Skin Inflammation in Mice

Journal of Investigative Dermatology (2017) **137,** 528–531; doi:10.1016/j.jid.2016.09.018

TO THE EDITOR

Imiquimod (IMQ) acts as a toll-like-receptor-7/8 agonist and its topical application is used as a model for psoriasiform skin inflammation. In mice and humans, skin inflammation is characterized by infiltration of several immune cells (Drobits et al., 2012; Kalb et al., 2012; Palamara et al., 2004) and activation of the IL-23/IL-17/IL-22 axis (Riol-Blanco et al., 2014; van der Fits et al., 2009). Major histocompatibility complex-II upregulation on keratinocytes, hyperproliferation, parakeratosis, and increased vascularization are also observed recapitulating psoriatic hallmarks (Flutter and Nestle, 2013).

Hair removal is essential before IMQ is applied to the murine skin. Different laboratories use various depilation strategies such as razor shaving, depilation cream, or wax stripping. Shaving

Abbreviations: HF, hair follicle; IF, infundibulum; IFE, interfollicular epidermis; IMQ, imiquimod

Accepted manuscript published online 30 September 2016; corrected proof published online 30 November 2016